

The Density Profile of the Dark Matter Halo of NGC 4605

Alberto D. Bolatto, Joshua D. Simon, Adam Leroy, and Leo Blitz
*Department of Astronomy, University of California at Berkeley,
 601 Campbell Hall MC 3411, CA 94720*
 bolatto@astro.berkeley.edu

ABSTRACT

We have obtained ~ 100 pc resolution CO and ~ 60 pc resolution H α observations of the dwarf spiral galaxy NGC 4605. We use them to derive a high resolution rotation curve and study the central density profile of NGC 4605's dark matter halo. We find that these observations do not agree with the predictions of most high resolution Cold Dark Matter calculations. We investigate two extreme cases: 1) NGC 4605 has a maximal exponential disk, that we model using K -band observations and remove to study the structure of its dark matter halo, and 2) NGC 4605 is dark matter dominated and its disk is dynamically negligible. Because the mass-to-light ratio of the maximal disk is already very low we favor the first solution, which indicates the halo has one component with a density profile $\rho \propto r^{-0.65}$ out to $R \sim 2.8$ kpc. In the second case, the rotation curve requires the presence of two components: a small (~ 600 pc) core surrounded by a much steeper $\rho \propto r^{-1.1}$ halo. Removal of intermediate (submaximal) disks does not ameliorate the discrepancy between the predictions and the observations.

1. Introduction

The Cold Dark Matter (CDM) paradigm and its variations (e.g., Λ CDM) have enjoyed remarkable success at explaining the large scale structure of the Universe. At the scale of individual galaxies, however, CDM faces several serious challenges (e.g., Sellwood & Kosowski 2000). One of the key predictions of CDM and Λ CDM simulations is that all dark matter halos share a universal density profile (Navarro, Frenk, & White 1996; Huss, Jain, & Steinmetz 1999). The original calculations predicted a central density profile $\rho \sim r^{-1}$, where r is the galactocentric distance. More recent, higher resolution simulations have found even steeper $\rho \sim r^{-1.5}$ central cusps (e.g., Moore et al. 1999; Ghigna et al. 2000).

These calculations, however, collide with a number of observational studies of dark-matter density profiles. Most of the observations find either central constant density cores (e.g., Flores & Primack 1994; McGaugh & de Blok 1998; de Blok et al. 2001; Borriello & Salucci 2001), or profiles where the density increases more slowly than r^{-1} toward the center (e.g., Kravtsov et al. 1998).

Other authors conclude that the observational evidence available to date is inconclusive, largely due to the lack of high quality high resolution rotation curves (van den Bosch et al. 2000). Indeed, using H I interferometers to obtain rotation curve data with the angular resolution and sensitivity required in order to resolve the central cusps is a daunting task for all but the nearest galaxies. The usual alternative, deriving rotation curves from longslit H α spectra, provides spatial information only along one dimension. This makes it impossible to separate circular and non circular motions and to check for position angle errors. Other potential problems with rotation curves based solely on H α are the systematic effects introduced by extinction and the local expansion flow of H II regions, which are especially important close to galaxy centers, precisely where the shape of the rotation curve is most important. A recent study by Blais-Ouellette, Amram, & Carignan (2001), however, shows good agreement between the measured H I and H α kinematics in the inner parts of their galaxies, indicating that at least in some galaxies extinction is not a substantial concern. Despite the recent body of work on the subject,

it remains clear that we need more high quality, high resolution rotation curve measurements to advance towards solving the galactic scale dark matter puzzle.

Since both H I and H α rotation curve studies are problematic, we have opted for a third, complementary technique: we use CO interferometry to measure the inner rotation curves. Millimeter wave interferometry avoids the problems inherent to the first two techniques. First, it is much more sensitive to surface brightness than H I interferometry, allowing us to routinely obtain sensitive data with 5'' angular resolution or better while the typical resolution of most H I studies is $\sim 30''$. Second, not only is CO interferometry unaffected by extinction, but it works best near galaxy centers where most molecular clouds are typically found. Third, like H I interferometry but unlike long slit H α spectroscopy, it provides complete spectral imaging information allowing us to obtain reliable rotation curves.

The relative sensitivity advantage of CO interferometry stems from the fact that the ^{12}CO ($J = 1 \rightarrow 0$) rotational transition at 2.6 mm has a wavelength ~ 80 times smaller than the 21 cm spin flip H I transition. This allows the CO antennas to be placed ~ 80 times closer together than the H I antennas for the same angular resolution. Because the sensitivity of aperture synthesis to surface brightness is proportional to the fraction of the filled aperture, compactness confers a considerable sensitivity advantage to millimeter wave interferometers. For example, the ten element Berkeley–Illinois–Maryland Association millimeter array (BIMA; Welch et al. 1996) has a 250 times larger filled aperture fraction than the VLA.

The difficulty in using CO interferometry for dark matter studies, however, is finding suitable target galaxies. Late type dwarf galaxies are ideal for such studies, because their density profiles are dominated by dark matter in their inner regions (Persic & Salucci 1990; Salucci, Ashman, & Persic 1991). Although little is known about the molecular gas content of most dwarf galaxies, with a few notable exceptions they are not strong molecular sources. We have obtained CO interferometer maps of several nearby dwarf galaxies with single-dish detections, a subset of which we selected for rotation curve studies. To further expand the set of suitable sources we are carrying out a system-

atic survey of nearby dwarf galaxies in CO. Thus, we expect that the results presented here are only a first glimpse of the final study. We present our observations in §2, perform a rotation curve study in §3, and summarize our results in §4.

2. Observations and Data Processing

The source we discuss in this work, NGC 4605, is an SBc dwarf galaxy. Independent photometric estimates place this galaxy ~ 4.6 Mpc (Karachentsev & Tikhonov 1994) and 4.26 ± 0.64 Mpc away (M. Pierce, priv. comm.), yielding a physical scale of ~ 20 pc'''. The physical resolution of our CO observations (and of our rotation curve) is therefore ~ 100 pc. The extinction corrected absolute B magnitude of NGC 4605 is $M_B = -18.10$ and its size is $R_{25} \sim 3'$ (~ 3.6 kpc), very similar to the magnitude and size of the Large Magellanic Cloud (LMC). The line-of-sight inclination of NGC 4605 is $i \approx 69$ deg, and H I observations find an inclination corrected linewidth at 20% intensity $W_{20} \approx 198$ km s $^{-1}$ (Bottinelli et al. 1985). This indicates a maximum rotational velocity of ~ 100 km s $^{-1}$ (again, similar to that of the LMC) that along with its size and luminosity definitively identifies this galaxy as a dwarf. Carbon monoxide millimeter emission was detected in NGC 4605 by Young et al. (1995) using the FCRAO 14 m radio telescope. Our first interferometer maps revealed CO emission throughout the disk of NGC 4605, which became the obvious first choice for a rotation curve study.

We observed the ^{12}CO ($J = 1 \rightarrow 0$) rotational transition in NGC 4605 using three configurations of the BIMA array (B, C, and D) between June 2000 and March 2001. We mapped one BIMA primary beam, subtending a field with a half power diameter of $\sim 100''$, sufficient to encompass the CO emission. The spectrometer was configured with 2 km s $^{-1}$ wide channels and a bandpass of 260 km s $^{-1}$. The individual tracks were calibrated, combined, imaged, and deconvolved using the CLEAN algorithm within the MIRIAD astronomical package. The resulting naturally weighted map has a beam size of $4.8'' \times 5.4''$ ($\sim 99 \times 111$ pc) with $P.A. \approx 6$ deg (Fig. 1). The individual planes of the datacube have an RMS of ~ 24 mJy beam $^{-1}$ (~ 85 mK) at a velocity resolution of 3 km s $^{-1}$.

The datacube was used to produce a first moment map of the CO emission (Fig. 2). The map was rotated to align the optical major axis of the galaxy with one of the coordinate axes ($P.A. = 125$ deg), and deprojected using the optical center and inclination angle. The velocity data were corrected by the sine of inclination angle, and sorted in concentric rings of width $5''$. To each ring we fit a model $v_{obs} = v_t + v_c \cos \theta + v_r \sin \theta$, representing the projected effects of translation (v_t), circular (v_c), and radial (v_r) velocities. The errors in the velocity map, multiplied by the square root of the beam oversampling factor, are used to weight each point in the fit (Fig. 3). The error bars for the fits (which range from 1.4 to 3.6 km s^{-1}) are computed using the diagonal of the covariance matrix. We find a small v_r component, increasing outwards to $\sim 25''$ and then leveling off (Fig. 4). This component is never larger than half v_c , and adding it in quadrature to v_c does not significantly change the density profile exponents discussed in this paper. The presence of this component may indicate that the kinematics inside $\sim 25''$ have a position angle slightly different from the optical $P.A.$ (closer to $P.A. \sim 95$ deg).

To extend the CO rotation curve beyond $50''$ (~ 1 kpc), we observed NGC 4605 with the 0.6 m Coudé Auxiliary Telescope at Lick Observatory on the night of 23 April 2001. We used the Hamilton Echelle Spectrometer with a 75\AA wide filter centered on $\text{H}\alpha$ ($\lambda = 6562.8\text{\AA}$) to block adjacent spectral orders. The slit was $640 \mu\text{m}$ ($6''$) wide and $\sim 8'$ long, oriented along NGC 4605's major axis at $P.A. = 125$ deg using the facility's focal plane image rotator. Our velocity resolution was $\sim 6 \text{ km s}^{-1}$, with a spatial resolution of $\sim 3''$. This spectral resolution is much higher than that of most published rotation curve studies, and it allows us to very accurately measure the kinematics of the inner disk of NGC 4605. We integrated for 4.5 hours divided in 30 minute exposures using manual guiding.

We reduced the $\text{H}\alpha$ data using IRAF. We removed a bias frame from the individual exposures, and combined them using the IMCOMBINE routine with its built in cosmic ray rejection algorithm. Because no continuum was detected in the individual images, we registered them using offsets obtained by cross correlating the spectra. For wavelength calibration we used exposures of

a ThAr reference lamp, and observations of a radial velocity standard star. To extract the rotation velocities we fit a gaussian to each row of the spectrum. We folded the results into a rotation curve by defining the center of the galaxy to be the point at which the two sides of the rotation curve lined up best. The typical errors in the individual points of the folded rotation curve were less than 2 km s^{-1} . Comparison of the CO and $\text{H}\alpha$ rotation data reveals that both tracers are in good agreement over the common region (Fig. 4). Thus $\text{H}\alpha$ appears to be a good tracer of the kinematics of the inner disk in NGC 4605.

We developed a simulation to estimate how our finite angular resolution affects both the CO and $\text{H}\alpha$ rotation curves (beam smearing). Because calculating the effect of the beam smearing requires assuming an underlying velocity field, we performed these computations in an iterative, self consistent manner. The net effect is very small, amounting to a velocity loss of $\sim 2 \text{ km s}^{-1}$ for the innermost points and rapidly decreasing outwards. Although small, this systematic velocity loss is not entirely negligible in the inner $30''$. We removed the effect of beam smearing from the data before performing the fits.

We used 2MASS K_s data to derive the distribution of mass in the disk of NGC 4605. The advantage of using K -band observations to model the disk mass over more typical B , V , or I data cannot be overemphasized: at K -band the extinction is a factor of ~ 10 down from V , and a factor of ~ 5 down from I (Rieke & Lebofsky 1985). We retrieved the archival 2MASS atlas image for NGC 4605 and extracted the surface brightness profile using the photometric calibration provided in the FITS header. We then fit an exponential disk to the surface brightness profile using data with galactocentric radii $r \in [10'', 60'']$, finding $\mu_K \approx 16.35 + 0.029 r$ where μ_K is the apparent K -band magnitude. NGC 4605 does not have a significant bulge, and the surface brightness distribution is well fit by an exponential law over this range.

3. Results and Discussion

The universal dark matter halo density law proposed by Navarro, Frenk, & White (1995) follows the form

$$\frac{\rho(r)}{\rho_{crit}} = \frac{\delta_c}{(r/r_s)(1+r/r_s)^2}, \quad (1)$$

where $\rho_{crit} = 3H^2/8\pi G \sim 1 \times 10^{-29} \text{ g cm}^{-3}$ is the critical density, δ_c is the halo overdensity, and r_s is the characteristic radius (simulations suggest r_s of several kpc). At galactocentric distances $r \ll r_s$ the halo has an approximate density profile $\rho \approx \rho_{crit} \delta_c r_s r^{-1}$. In general, a density profile $\rho \propto r^{-\alpha}$ implies

$$v_c \propto r^{(2-\alpha)/2}. \quad (2)$$

Most dark matter density profile studies assume that the halo is the dominant mass component, and do not attempt to model and remove the contribution from the galactic disk to the rotation, which is taken to be negligible. We call this approach the “minimal disk” hypothesis, since it implies that the mass-to-light (M/L) ratio of the material in the disk is $M/L \sim 0$. The opposite limit is given by the “maximal disk”; the maximum exponential disk that can be subtracted from the measured rotation curve without creating negative residual velocities. Fitting a maximal disk to the rotation curve yields a maximum mass-to-light ratio for the material in the disk (predominantly stars and gas).

To find the upper limit to the M/L ratio in NGC 4605 we fit a thin maximal exponential disk using our rotation curve and the 2MASS K -band data. The fit is constrained by the innermost points of the rotation measurements. This fit yields $M/L_K = 0.25 \pm 0.03 M_\odot/L_{\odot K}$ (we assume $M_{\odot K} = 3.34$), implying a disk mass surface density of stars plus gas $\mu = 0.053 \exp(-r/37''1) \text{ g cm}^{-2}$. The extinction corrected color, $B - R = 0.67$ (M. Pierce, priv. comm.), predicts a similar mass-to-light ratio $M/L_K \sim 0.34$ (Bell & de Jong 2001). This value is very close to the lower limit of the reasonable range of M/L_K , possibly corresponding to a young starburst population according to the Starburst99 models (Leitherer et al. 1999). This idea is further supported by the observation that, in dwarf galaxies, bright CO emission appears to be accompanied by the intense star formation activity signaling a young starburst. The fact that the upper limit of M/L is so low suggests that the disk of NGC 4605 is quite close to maximal, as submaximal disks will imply even lower

values of the mass-to-light ratio. Using the single dish CO and H I data and allowing for Magellanic metallicities we estimate the gas is $\sim 20\%$ of the total mass of the maximal disk. The effect of including the gas would be to lower the stellar mass-to-light ratio to $M/L_K \sim 0.20 M_\odot/L_{\odot K}$. Because this correction is somewhat uncertain we ignore it in the following discussion, but note that its only effect is to make the M/L ratio even lower.

The rotation due to an exponential disk is straightforward to compute (Freeman 1970), and to remove it from the measured rotation we use $v_c^2 = v_{halo}^2 + v_{disk}^2$, where all velocities are circular velocities (Binney & Tremaine 1987). Figure 5 shows the result of removing the maximal disk contribution from the overall rotation. To the residual rotation, due to the halo, we fit a $v_{halo} \propto r^\beta$ power law in the region $r \in [40'', 140'']$ and find the corresponding α using Eq. 2. The best fit power law is $v_c \sim 3.0 r^{0.67} \text{ km s}^{-1}$, implying $\rho \sim 4.9 \times 10^{-24} R^{-0.65} \text{ g cm}^{-3}$ (where R is the galactocentric radius in kpc). This value of α is significantly lower than the calculations by Navarro et al. (1996) or Moore et al. (1999) indicate. Note, however, that it agrees well with the critical solution recently found by Taylor & Navarro (2001) with $\alpha \sim 0.75$. Thus, *removing the maximal disk from the rotation curve of NGC 4605 results in a shallow halo, with a density exponent $\alpha = 0.65 \pm 0.02$* . The error bars including the uncertainty in the M/L ratio are ± 0.07 .

It is interesting to investigate whether the halo rotation of NGC 4605 shows any hint of a constant density core, such as those proposed for other galaxies (e.g., Borriello & Salucci 2001). The region inward of $30''$ in Fig. 5b does not show a significant departure from the outer halo fit, especially after correcting the innermost points for the effects of beam smearing. While most velocity residuals inside $30''$ are negative, the overall deficit is less than 2 km s^{-1} . Because the maximal disk is dynamically dominant inside $r = 40''$ any departures from a perfect exponential disk, or from a constant mass-to-light ratio, can account for it. Among other problems that could introduce similar systematic errors near the centers of galaxies are: 1) a displacement of the H α slit by a few arcseconds perpendicular to the major axis of the galaxy, 2) a disagreement of a few arcseconds between the optical and dynamical centers, or 3)

the presence of a weak galactic bar with the consequent non circular orbits. For these reasons, it is difficult to completely exclude a constant density core using these data: in the presence of a dynamically dominant disk the rotational signature of such core is a deficit of a few km s^{-1} throughout this region. Thus, although we find no evidence for a constant density core, we cannot discard it completely.

What happens if despite the evidence for a maximal disk in NGC 4605 we assume the minimal disk hypothesis? It is easy to see that the observed rotation cannot be fit well by a single power law (Fig. 4). This suggests that there are at least two distinct mass components that are contributing to the potential. Indeed, a possible decomposition of the rotation curve of NGC 4605 indicates a slowly varying density profile inside $30''$ (i.e., a core with $v_c \sim 3.0 r^{0.8} \text{ km s}^{-1}$, implying $\rho \sim 1.5 \times 10^{-23} R^{-0.4} \text{ g cm}^{-3}$), and a rapidly decreasing density outwards of $40''$ ($v_c \sim 10.4 r^{0.45} \text{ km s}^{-1}$, yielding $\rho \sim 8 \times 10^{-24} R^{-1.1} \text{ g cm}^{-3}$). *In the absence of a disk the observed rotation requires a two component halo: a core with $\alpha = 0.4 \pm 0.2$ inside $r \sim 30''$ and an outer halo with $\alpha = 1.1 \pm 0.02$.*

Both of these limits are in disagreement with most results of collisionless cold dark matter simulations. The removal of a submaximal disk does not eliminate the discrepancy. Such a solution has a combination of the problems of each limit, requiring both a shallow outer halo and an inner core. It should be noted that the goodness of fit of the outer halo by a power law (or any other mathematical model used to describe it) cannot be reliably employed to obtain a “best fit” mass-to-light ratio and select a solution. Indeed, we find that for M/L in the range $M/L \in [0, 0.25] M_\odot/L_{\odot K}$, the RMS of the residuals of the power law fit to the rotation curve only changes from 1.5 (Fig. 4b) to 1.9 km s^{-1} (Fig. 5b), showing that the RMS is very insensitive to how much of the stellar disk is removed. We have argued that, because we find a low mass-to-light ratio, NGC 4605’s disk is close to maximal. This solution has the virtue of requiring only one halo component. Regardless of the precise M/L ratio of the disk of NGC 4605, the inescapable conclusion is that the shape of the halo of NGC 4605 poses a challenge to the CDM simulations.

4. Summary and Conclusions

We have measured the kinematics of the dwarf galaxy NGC 4605 with high spectral ($\sim 2 \text{ km s}^{-1}$ for the CO, $\sim 6 \text{ km s}^{-1}$ for the H α) and spatial ($\sim 100 \text{ pc}$) resolution. Our study of the combined CO and H α rotation curve leads to a robust conclusion: the standard collisionless CDM simulations do not accurately predict its shape. We have discussed two extreme cases: 1) the measured rotation is due to a combination of the halo and an exponential maximal disk, and 2) the rotation is due to solely the halo (i.e., the minimal disk hypothesis). Because the K -band mass-to-light ratio we find for the first case is very low ($M/L_K \approx 0.25 M_\odot/L_{\odot K}$), we believe that the disk of NGC 4605 is close to maximal and that the first solution is the correct one. This solution requires only one halo component within $R \sim 2.8 \text{ kpc}$. The resulting $\rho \sim r^{-\alpha}$ halo density profile has $\alpha = 0.65 \pm 0.07$. This exponent is substantially lower than the predictions of most high resolution CDM calculations, although it agrees much better with the critical solution found by Taylor & Navarro (2001).

If we disregard the evidence favoring a maximal disk and adopt the minimal disk case, we find that we need a soft $\rho \sim r^{-0.4}$ core to explain the rotation of the innermost 600 pc. Note that while the precise value of α for this core is rather uncertain, the fact that a break in α is required is not. Furthermore, the density profile of the halo in the 0.8 to 2.8 kpc region has $\alpha = 1.1 \pm 0.02$. This is still noticeably different from the results of some of the recent high resolution simulations which find $\alpha \approx 1.5$ (Moore et al. 1999; Ghigna et al. 2000), although it agrees with other calculations that find $\alpha \approx 1.1$ (Jing & Suto 2000). None of these calculations, however, predict the core. The removal of a submaximal disk has a combination of the problems of these two extreme cases.

Notwithstanding which solution is the best, both of these extremes (and all of the intermediate cases) are discrepant with most of the available predictions of standard CDM. We have to note that the strength of these conclusions stems from the fact that both the CO and the H α data, independently, reveal the same kinematics for the inner $50''$ of NGC 4605. A similar analysis, relying only on one or the other rotation curves, would

be impaired by the possible systematics of the individual datasets.

We wish to thank the anonymous referee for a speedy and thorough review of this paper. We wish to acknowledge the help of James Graham, and the support of the RAL and the BIMA team, especially R. Forster, R. Gruendl, R. Plambeck, and E. Sutton. This research was supported by NSF grant AST-9981308, and made extensive use of the NASA/IPAC Extragalactic Database (NED), the Los Alamos National Laboratory astrophysics preprint database, and NASA's Astrophysics Data System Abstract Service (ADS).

REFERENCES

- Bell, E. F., & de Jong, R. S. 2001, *ApJ*, 550, 212
- Binney, J., & Tremaine, S. 1987, *Galactic Dynamics* (Princeton, NJ : Princeton University Press)
- Blais-Ouellette, S., Amram, P., & Carignan, C. 2001, *AJ*, 121, 1952
- de Blok, W. J. G., McGaugh, S. S., Bosma, A., & Rubin, V. C. 2001, *astro-ph/0103102*
- Borriello, A., & Salucci, P. 2001, *MNRAS*, 323, 285
- van den Bosch, F. C., Robertson, B. E., Dalcanton, J. J., & de Blok, W. J. G. 2000, *AJ*, 119, 1579
- Bottinelli, L., Gougenheim, L., Paturel, G., & de Vaucouleurs G. 1985, *A&AS*, 59, 43
- Flores, R. A. & Primack, J. R. 1994, *ApJ*, 427, L1
- Freeman, K. C. 1970, *ApJ*, 160, 811
- Ghigna, S., Moore, B., Governato, F., Lake, G., Quinn, T., & Stadel, J. 2000, *ApJ*, 544, 616
- Huss, A., Jain, B., & Steinmetz, M. 1999, *ApJ*, 517, 64
- Jing, Y. P., & Suto, Y. 2000, *ApJ*, 529, L69
- Karachentsev, I. D., & Tikhonov, N. A. 1994, *A&A*, 286, 718
- Kravtsov, A. V., Klypin, A. A., Bullock, J. S., & Primack, J. R. 1998, *ApJ*, 502, 48
- Leitherer et al. 1999, *ApJS*, 123, 3
- McGaugh, S. S. & de Blok, W. J. G. 1998, *ApJ*, 499, 41
- Moore, B., Ghigna, S., Governato, F., Lake, G., Quinn, T., Stadel, J., & Tozzi, P. 1999, *ApJ*, 524, L19
- Navarro, J. F., Frenk, C. S., & White, S. D. M. 1995, *MNRAS*, 275, 720
- Navarro, J. F., Frenk, C. S., & White, S. D. M. 1996, *ApJ*, 462, 563
- Persic, M. & Salucci, P. 1990, *MNRAS*, 245, 577
- Rieke, G. H., & Lebofsky, M. J. 1985, *ApJ*, 288, 618
- Salucci, P., Ashman, K. M., & Persic, M. 1991, *ApJ*, 379, 89
- Sellwood, J. A., & Kosowski, A. 2000, in *Gas & Galaxy Evolution*, eds. Hibbard, Rupen, & van Gorkom, *astro-ph/0009074*
- Taylor, J. E., & Navarro, J. F. 2001, *ApJ*, submitted (*astro-ph/0104002*)
- Welch, W. J. et al. 1996, *PASP*, 108, 93
- Young, J. S., et al. 1995, *ApJSS*, 98, 219

This 2-column preprint was prepared with the AAS L^AT_EX macros v5.0.

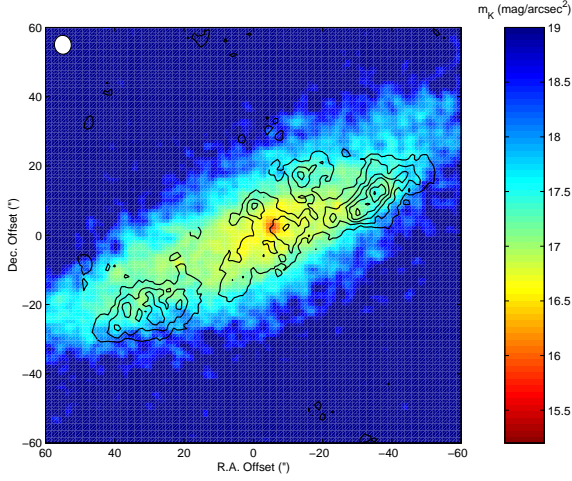


Fig. 1.— 2MASS K -band image of NGC 4605 with integrated intensity CO contours overlaid. The RMS of the integrated intensity data is ~ 130 mJy beam $^{-1}$ km s $^{-1}$ (~ 450 mK km s $^{-1}$). The contours start at 3σ and increase in steps of 4σ to 3 Jy beam $^{-1}$ km s $^{-1}$. The offsets are with respect to NGC 4605's center, at $\alpha_{J2000} = 12^{\text{h}}40^{\text{m}}00^{\text{s}}.0$, $\delta_{J2000} = 61^{\circ}36'31''$. The synthesized beam is shown in the upper left corner.

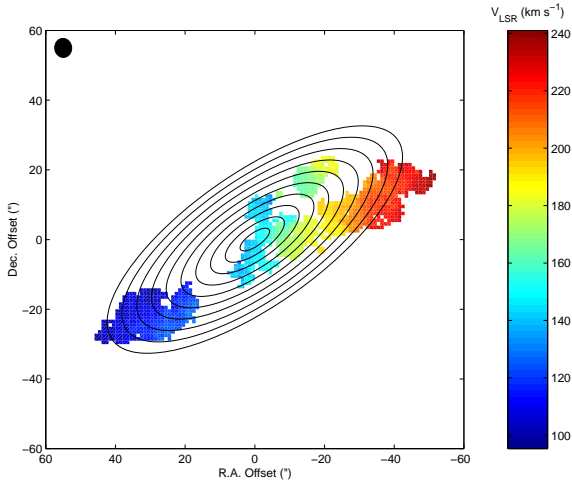


Fig. 2.— Velocity field obtained from the CO datacube. The typical 1σ error in the velocities is $\sim 2 - 3$ km s $^{-1}$. The ellipses correspond to the projection of the $5''$ wide rings used to determine the rotation curve.

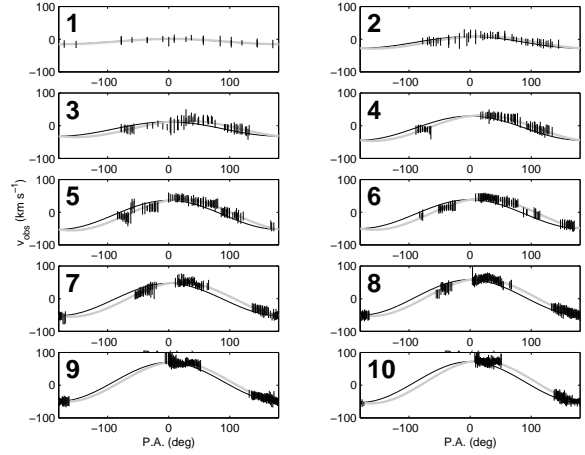


Fig. 3.— Individual fits to the CO rings, velocity plotted against angle. The number in the upper left corner indicates the ring number, increasing outwards. The vertical lines are the individual data points with their errors, including the square root of oversampling factor. The gray thick line is the overall fit to v_{obs} , while the black thin line is the v_c component, as described in the main text.

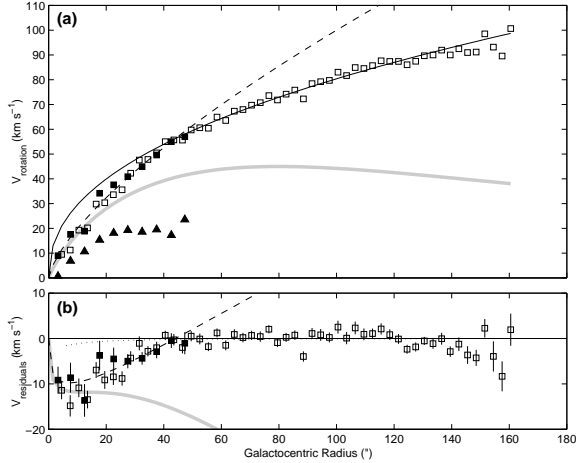


Fig. 4.— Combined CO and H α rotation curve of NGC 4605 with no disk removed, in linear–linear scale. Plot (a) shows the individual rotation measurements for CO (filled squares) and H α (open squares). It also shows the v_r component obtained from the CO (filled triangles). The CO is sampled every 5'', the H α every 3'', and both have been corrected for the effects of beam smearing. The solid line is the power law fit to the outer halo H α data in the $r \in [40'', 140'']$ region, $\rho \propto r^{-1.1}$. The dashed line is the power law fit to the CO rotation, yielding $\rho \propto r^{-0.6}$. The gray thick line is the maximal disk obtained from the K -band observations. Plot (b) shows the residuals in the data and the fits, after removing the outer halo fit. The dotted line is the effect of beam smearing, as it was removed from the H α observations. The correction applied to the CO data is very similar. The error bars are internal, statistical errors obtained from the fits.

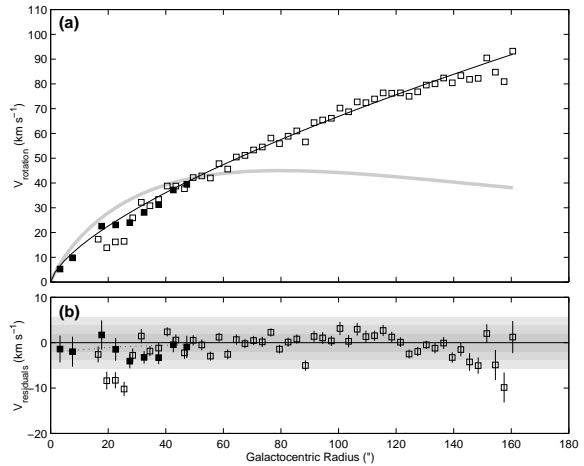


Fig. 5.— Combined CO and H α rotation curve of NGC 4605 after removing the maximal disk. The key to symbols and lines is the same as in Fig. 4. The few data points missing had $v_c < v_{disk}$, yielding imaginary v_{halo} . Plot (a) shows the new outer halo fit for $r \in [40'', 140'']$, $\rho \propto r^{-0.65}$, and the fact that the maximal disk is dynamically dominant inside $r \sim 50''$. Plot (b) shows the residuals after removing the outer halo fit. The gray regions indicate 1σ , 2σ , and 3σ departures from the fit. There is no evidence for a break in the power law (i.e., a core) after the disk is removed.